

# Under Water Image Enhancement By The Multilevel Fusion

M. Sri Lakshmi<sup>1</sup>, V. Balaji<sup>2</sup>

<sup>1</sup>Dept of Digital image processing

<sup>2</sup>Assistant Professor, Dept of CSE

<sup>1,2</sup> Acharya Nagarjuna University, Andhra Pradesh

**Abstract-** Image enhancement is a process of increasing the clarity of image by its characteristics. Identification of the object inside the water is difficult because of the poor contrast and visibility. Here we used recent methods that are developed for the underwater environment. The mingle of two images that are derived from color remunerated and white-balanced approximation of the old degraded image. The two images to fusion, as well as their related weight maps, are defined to transfer of edges and color contrast to the output. Gamma correction is used to alter the output levels of a monitor. To avoid the sharp weight map transitions create surface in the low frequency components of the reconstructed image, here we use multi scale fusion strategy. Fusion gives the result of the dark regions, increase the global contrast and edge sharpness. By using this algorithm the output is independent of the camera settings as well as it increases the accuracy of image processing applications that is image segmentation and key point matching.

**Keywords-** Underwater, image fusion, white-balancing.

## I. INTRODUCTION

Upgrading the quality of the image is nothing but the image enhancement. In the sea water images, the objects at a distance of more than 10 meters are unperceivable and the colors are faded because their composing wavelengths are cut according to the water depth. Underwater image is an important source in different branches of technology and scientific research, such as inspection of underwater infrastructures and cables, detection of man-made objects, control of underwater vehicles, marine biology research, and archeology. The presence of the floating particles are known as “marine snow” increase absorption and scattering effects. The main components of fusion based enhancing technique, including inputs and associated weight maps. Before concluding comparative qualitative and quantitative assessments of our white-balancing and fusion-based underwater dehazing techniques, as well as some results about their relevance to address common computer vision problems, namely image segmentation and feature matching. The dark channel prior is based on the following observation on turbid free or haze-free images: In most of the patches, at least one

among the three color channel (R, G, and B) has some pixels whose intensity are very low and close to zero. Due to the reason of having shortest wavelength of blue color it can travels a long distance results more dominant than other color in water. Our approach is focusing on recovery of degraded image followed by enhancement. Proposed methodology is related to dark channel prior phenomenon. DCP use the information to remove the haze and color variations based on color compensation. The DCP has initially been proposed for outdoor scenes dehazing. It assumes that the radiance of an object in a natural scene is small in at least one of the color component, and consequently defines regions of small transmission as the ones with large minimal value of colors.

## II. BACKGROUND KNOWLEDGE

In this we have been considered to restore or enhance the images captured in the under water. In this first section, discuss about the white balancing for increasing the contrast of the image. In this second section, discuss about the gamma correction for controls the overall brightness of an image. In this third section, discuss about the sharpening for subtract a blurred copy to detect the edges. In this third section, discuss about the multi-scale fusion for balancing the weights.

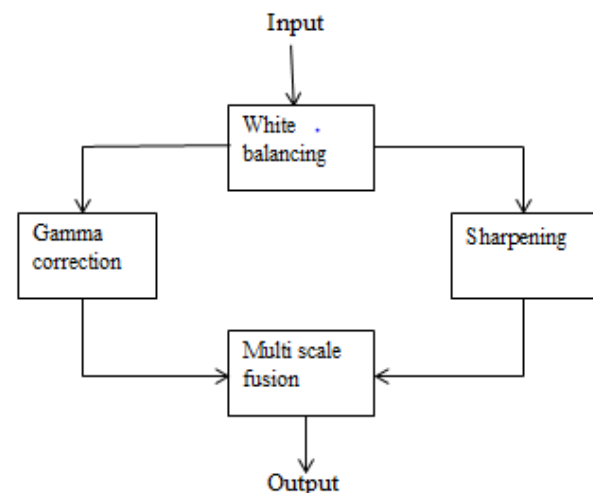


**Fig1. Designing of multi-scale fusion**

### 2.1 White balancing:

The white balancing step aims to removing the color cast induced by the underwater light scattering. The input image is taken from the underwater to perform the white balancing. White balancing is reduces the contrast of the image present in the dark channel. The image splits into two inputs LF and RF then pass to the next section.



Fig.2 White balancing

## 2.2 Gamma correction:

Gamma correction controls the brightness of an image. Images which are not properly corrected can look either bleached out, or too dark. Gamma correction takes the input from white balancing (LF) and performs the gamma correction to reduce the darkness present in the image.

## 2.3 Sharpening:

Sharpening is the process of refining a sharp edge of appropriate shape on a tool. We discuss about the sharpening for subtract a blurred copy to detect the edges. The input from the white balancing (RF) is passing to the sharpening to the edges. Shading is also reduced by the sharpening for better visual effects.

## 2.4 Multi scale fusion:

Two images are derived from a white-balanced version of the single input, and are merged based on a (standard) multi-scale fusion algorithm. By using this we avoid the noise present in the image. Weight is balanced by the fusion.

Digital image processing is the processing of manipulation of digital image through a digital computer.

## Light Propagation in Underwater

The interaction between the surface and the source light is affected by the time of the day, shape of the interface between the water and air (rough vs. calm sea). When the light

is propagates on the water it reflects back and some energy is observed. In sea water the light has to go through is several hundreds of times than in normal atmosphere. In deeper oceans green and blue colors are not effective because of the dark channel prior. As phenomenon, sub sea water absorbs step by step different wavelengths of light. Red, which corresponds to the longest wavelength, is the first to be absorbed (10-15ft), followed by orange (20-25ft) and yellow (35-45ft). The loss of red is noticeable in the pictures up to the 5ft. The underwater objects can appear 25% more than the reality.

The comprehensive studies of McGlamery [12] and Jaffe [13] have shown that the total irradiance incident on a generic point of the image plane has three main components in underwater mediums: direct component, forward scattering and back scattering. The direct component is the component of light source is reflected directly by the target object onto the image plane. The image coordinate  $X$  is the direct component is expressed as:

$$E_D(x) = J(x)e^{-\eta d(x)} = J(x)t(x) \quad (1)$$

Where  $J(x)$  is the radiance of the object,  $d(x)$  is the distance between the observer and the object, and  $\eta$  is the attenuation coefficient. The exponential term  $e^{-\eta d(x)}$  is also known as the transmission  $t(x)$  through the underwater medium.

When the flash hits the water particles, and it's reflect back to the camera. It simply changes the position and angle of the image pixels. Because of this back scattering the contrast loss and color changes is happened.

Mathematically, it is often expressed as:

$$E_{BS}(x) = B_{\infty}(x) (1 - e^{-\eta d(x)}) \quad (2)$$

Where,  $B_{\infty}(x)$  is a color vector known as the back scattered light. Ignoring the forward scattering component, the simplified underwater optical model thus becomes:

$$I(x) = J(x) e^{-\eta d(x)} + B_{\infty}(x) (1 - e^{-\eta d(x)}) \quad (3)$$

## III. PROPOSED SYSTEM

In image enhancement approach we adopts a two-step strategy, that is combining of white balancing and image fusion, to improve underwater images without resorting to the explicit inversion of the optical model. In our approach, white balancing aims at compensating for the color cast caused by the selective absorption of colors with depth, while image

fusion is considered to enhance the edges and details of the scene, to mitigate the loss of contrast resulting from backscattering. We now focus on the white-balancing stage. White-balancing aims at improving the image aspect, primarily by removing the undesired color castings due to various illumination or medium attenuation properties. In underwater, the perception of color is highly correlated with the depth, and an important problem is the green-bluish appearance that needs to be rectified. When the light pass through the water, the attenuation process affects selectively the wavelength spectrum, thus affecting the intensity and the appearance of a colored surface. Since the scattering attenuates more the long wavelengths than the short ones, the color perception is affected as we go down in deeper water. In practice, the attenuation and the loss of color also depends on the total distance between the observer and the scene

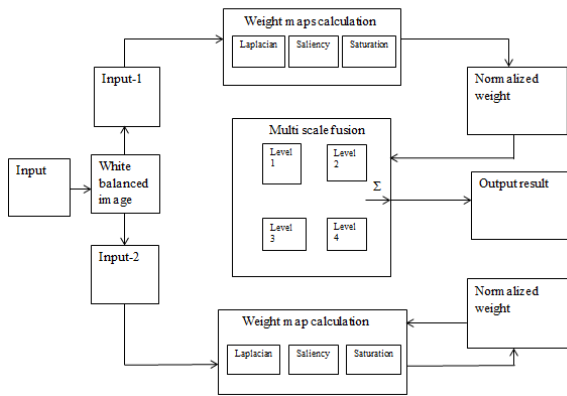


Fig3. Multi-scale fusion architecture

By this process bluish tone is gray world, but fails in the red artifacts because of the low mean values.

To compensate for the loss of red channel is:

1. The green channel is relatively well preserved in the under water, compared to the red and blue channels. Light with a long wavelength i.e. the red light, is indeed lost first when traveling in clear water;
2. The green channel consists opponent color information compared to the red channel and it is important to compensate for the stronger attenuation induced on red, compared to green one. Therefore, we compensate the red attenuation by adding a fraction of the green channel to red. We had initially tried to add both a fraction of green and blue to the red but, as can be observed in Fig. 3, using the information of the green channel allows to better recover the entire color spectrum while maintaining a natural appearance of the background;

3. The compensation must be proportional to the difference between the mean green and the mean red values because, under the Gray world assumption, this difference reflects the unbalance between red and green attenuation;
4. To avoid saturation of the red channel during the Gray World step that follows the red loss compensation, the enhancement of red should primarily affect the pixels with small red channel values, and should not change pixels that already include a significant red component. In other words, the green channel information should not be transferred in regions where the information of the red channel is still significant. Thereby, we want to avoid the reddish appearance introduced by the Gray-World algorithm in the over exposed regions. Basically, the compensation of the red channel has to be performed only in those regions that are highly attenuated. This argument follows the statement in, telling that if a pixel has a significant value for the three channels, this is because it lies in a location near the observer, or in an artificially illuminated area, and does not need to be restored.

Mathematically, express the compensated red channel  $I_{rc}$  at every pixel location  $(x)$  as follows:

$$I_{rc}(x) = I_r(x) + \alpha \cdot (\bar{I}_g - \bar{I}_r) \cdot (1 - I_r(x)) \cdot I_g(x), \tag{4}$$

where  $I_r$ ,  $I_g$  represent the red and green color channels of image  $I$ , each channel being in the interval  $[0, 1]$ , after normalization by the upper limit of their dynamic range; while  $\bar{I}_r$  and  $\bar{I}_g$  denote the mean value of  $I_r$  and  $I_g$ . In Equation 4, each factor in the second term directly results from one of the above observations, and  $\alpha$  denotes a constant parameter. In practice, our tests have revealed that a value of  $\alpha = 1$

To compute the compensated blue channel  $I_{bc}$  as:

$$I_{bc}(x) = I_b(x) + \alpha \cdot (\bar{I}_g - \bar{I}_b) \cdot (1 - I_b(x)) \cdot I_g(x), \tag{5}$$

Where  $I_b$ ,  $I_g$  represent the blue and green color channels of image  $I$ , and  $\alpha$  is also set to one. In the rest of the paper, the blue compensation is only considered in Figure 3. All other results are derived based on the sole red compensation.

After the red (and optionally the blue) channel attenuation has been compensated, we resort to the conventional Gray-World assumption to estimate and compensate the illuminant color cast.

### A. Inputs of the Fusion Process

To overcome this loss we perform the sharpened version of the white balanced image. Finally we follow the unsharp masking principle the formula for the unsharp masking gives the sharpened image  $S$ .

$$S = I + \beta (I - G * I), \quad (6)$$

Where  $I$  is the white balanced image  $G * I$  denotes the Gaussian filtered version of  $I$ , and  $\beta$  is a parameter. In practice, the selection of  $\beta$  is not trivial. A small  $\beta$  fails to sharpen  $I$ , but a too large  $\beta$  results in over-saturated regions, with brighter highlights and darker shadows. To circumvent this problem, we define the sharpened image  $S$  as follows:

$$S = (I + N \{I - G * I\})/2, \quad (7)$$

The sharpening method defined in (7) is referred to as normalized unsharp masking process. It has the advantage to not require any parameter tuning, and appears to be effective in terms of sharpening.

### B. Weights of the Fusion Process

Weight of the pixel is important to represent the image in a better way, based on the saliency metrics or number of local image quality.

#### 3.1 Laplacian contrast weight (WL):

Laplacian filter is applied on the luminance channel for estimates the global contrast. This indicator is used in many applications such as tone mapping and extending depth of field to assigns high values to edges and texture. This weight is not enough to recover the contrast for this we introduce complementary much between a ramp flat regions. To handle this problem, we contrast assessment metric.

**3.2 Saliency weight (Ws):** Saliency map is used for highlighted area by the high luminance values and regions. For this we used an additional weight map based on the observation that saturation decreases in the highlighted regions.

**3.3 Saturation weight (Wsat):** The weight map is simply computed (for each input  $I_k$ ) as the deviation (for every pixel

location) between the  $R_k$ ,  $G_k$  and  $B_k$  color channels and the luminance  $L_k$  of the  $k$ th input:

$$W_{sat} = [1/3(R_k - L_k)^2 + (G_k - L_k)^2 + (B_k - L_k)^2]^{1/2} \quad (8)$$

In practice, for each input, the three weight maps are merged in a single weight map as follows. For each input  $k$ , an aggregated weight map  $W_k$  is first obtained by summing up the three  $W_L$ ,  $W_S$ , and  $W_{sat}$  weight maps. The  $K$  aggregated maps are then normalized on a pixel-per-pixel basis, by dividing the weight of each pixel in each map by the sum of the weights of the same pixel over all maps. Formally, the normalized weight maps  $\overline{W_k}$  are computed for each input as

$$W_k = (W_k + \delta) / (K \sum_{k=1}^K W_k + K \cdot \delta), \quad (9)$$

With  $\delta$  denoting a small regularization term that ensures that each input contributes to the output.  $\delta$  is set to 0.1 in the rest of the paper. The normalized weights of corresponding weights are shown at the bottom of Fig.3.

To reducing the overall complexity of the fusion process, the sharpening image and gamma corrected image are combined and performs the fusion. Final output gives more information compare to the previous image.

## IV. RESULTS AND DISCUSSION

Then we canvas our dehazing method with the existing enhancement techniques. At last we prove the quality of the image is shown by using the MSE and PSNR values.

The mean square error (MSE) is the most widely used full reference quality, computed by averaging the squared intensity differences of distorted and reference image pixels, along with the related quantity of peak signal-to-noise ratio (PSNR). These are appealing because they are simple to calculate, have clear physical meanings, and are mathematically convenient in the context of optimization. The majority of the proposed perceptual quality assessment models have followed a strategy of modifying the MSE measure so that are penalized in accordance with their visibility. By using this we can directly derive how much of noise is reduced. The proposed method shows better results compared with the earlier methods.

Mathematically MSE and PSNR are represented as follows:



$$MSE = \frac{\sum_{i=1}^x \sum_{j=1}^y (|A_{ij} - B_{ij}|)}{x * y} \quad (10)$$

$A_{ij}$  -is original image,  $B_{ij}$  fused image

$x * y$  -are the rows and columns of the image

$$PSNR (dB) = 10 * \log \left( \frac{255^2}{MSE} \right) \quad (11)$$

The MSE and the PSNR are the two error metrics used to compare image compression quality.

**Table: 1 Reduced noise**

| Noise image | MSE   | PSNR  |
|-------------|-------|-------|
| Figure1     | 79.74 | 38.71 |
| Lena        | 81.28 | 34.80 |
| Fish        | 84.71 | 41.41 |

**Table:2 Noise present in the image**

| Noise image | MSE   | PSNR  |
|-------------|-------|-------|
| Figure1     | 79.74 | 38.71 |
| Lena        | 81.28 | 34.80 |
| Fish        | 84.71 | 41.41 |

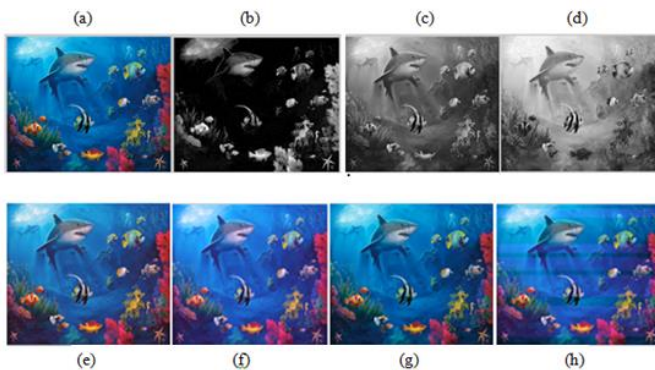


fig4.



Fig5

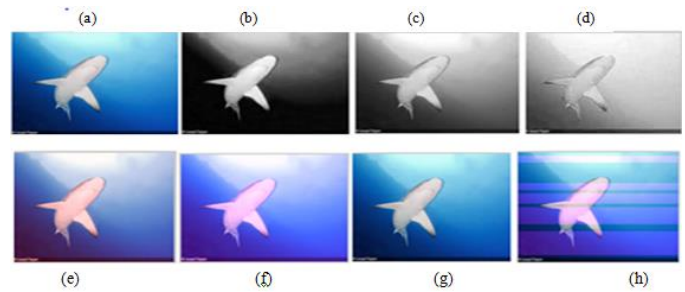


Fig6

Fig4,5,6: White balancing by (a)input image, (b)white balanced for red channel, (c)white balanced for green channel,(d)white balanced for blue channel, (e)gamma correction for red channel, (f)gamma correction for blue channel, (g)sharpening, (h)fused image.

## V. CONCLUSIONS

We used an alternate method to enhance the videos and images. Our approach builds on the fusion based on the single original image and able to enhance the wide range of underwater image. We demonstrate the utility and relevance of the proposed image enhancement technique for several challenging underwater computer vision applications.

## REFERENCES

- [1] M. D. Kocak, F. R. Dalglish, M. F. Caimi, and Y. Y. Schechner, "A focus on recent developments and trends in underwater imaging," *Marine Technol. Soc. J.*, vol. 42, no. 1, pp. 52–67, 2008.
- [2] G. L. Foresti, "Visual inspection of sea bottom structures by an autonomous underwater vehicle," *IEEE Trans. Syst., Man, Cybern. B, Cybern.*, vol. 31, no. 5, pp. 691–705, Oct. 2001.
- [3] A. Ortiz, M. Simó, and G. Oliver, "A vision system for an underwater cable tracker," *Mach. Vis. Appl.*, vol. 13, pp. 129–140, Jul. 2002.
- [4] A. Olmos and E. Trucco, "Detecting man-made objects in unconstrained subsea videos," in *Proc. BMVC*, Sep. 2002, pp. 1–10.
- [5] B. A. Levedahl and L. Silverberg, "Control of underwater vehicles in full unsteady flow," *IEEE J. Ocean. Eng.*, vol. 34, no. 4, pp. 656–668, Oct. 2009.
- [6] C. H. Mazel, "In situ measurement of reflectance and fluorescence spectra to support hyperspectral remote sensing and marine biology research," in *Proc. IEEE OCEANS*, Sep. 2006, pp. 1–4.
- [7] Y. Kahanov and J. G. Royal, "Analysis of hull remains of the Dor D Vessel, Tantura Lagoon, Israel," *Int. J. Nautical Archeol.*, vol. 30, pp. 257–265, Oct. 2001.

- [8] R. Schettini and S. Corchs, "Underwater image processing: state of the art of restoration and image enhancement methods," *EURASIP J. Adv. Signal Process.*, vol. 2010, Dec. 2010, Art. no. 746052.
- [9] S. G. Narasimhan and S. K. Nayar, "Contrast restoration of weather degraded images," *IEEE Trans. Pattern Anal. Mach. Learn.*, vol. 25, no. 6, pp. 713–724, Jun. 2003.
- [10] D.-M. He and G. G. L. Seet, "Divergent-beam LiDAR imaging in turbid water," *Opt. Lasers Eng.*, vol. 41, pp. 217–231, Jan. 2004.
- [11] Y. Y. Schechner and Y. Averbuch, "Regularized image recovery in scattering media," *IEEE Trans. Pattern Anal. Mach. Intell.*, vol. 29, no. 9, pp. 1655–1660, Sep. 2007.
- [12] B. L. McGlamery, "A computer model for underwater camera systems," *Proc. SPIE*, vol. 208, pp. 221–231, Oct. 1979.
- [13] J. S. Jaffe, "Computer modeling and the design of optimal underwater imaging systems," *IEEE J. Ocean. Eng.*, vol. 15, no. 2, pp. 101–111, Apr. 1990.
- [14] H. Koschmieder, "Theorie der horizontalen sichtweite," *Beitrage Phys. Freien Atmos.*, vol. 12, pp. 171–181, 1924.
- [15] M. Levoy, B. Chen, V. Vaish, M. Horowitz, I. McDowall, and M. Bolas, "Synthetic aperture confocal imaging," in *Proc. ACM SIGGRAPH*, Aug. 2004, pp. 825–834.
- [16] S. K. Nayar and S. G. Narasimhan, "Vision in bad weather," in *Proc. IEEE ICCV*, Sep. 1999, pp. 820–827.
- [17] J. Kopf et al., "Deep photo: Model-based photograph enhancement and viewing," *ACM Trans. Graph.*, vol. 27, Dec. 2008, Art. no. 116.
- [18] R. Fattal, "Single image dehazing," in *Proc. ACM SIGGRAPH*, Aug. 2008, Art. no. 72.
- [19] K. He, J. Sun, and X. Tang, "Single image haze removal using dark channel prior," in *Proc. IEEE CVPR*, Jun. 2009, pp. 1956–1963.
- [20] J.-P. Tarel and N. Hautiere, "Fast visibility restoration from a single color or gray level image," in *Proc. IEEE ICCV*, Sep. 2009, pp. 2201–2208.
- [21] J.-P. Tarel, N. Hautiere, L. Caraffa, A. Cord, H. Halmaoui, and D. Gruyer, "Vision enhancement in homogeneous and heterogeneous fog," *IEEE Intell. Transp. Syst. Mag.*, vol. 4, no. 2, pp. 6–20, Aug. 2012.
- [22] L. Kratz and K. Nishino, "Factorizing scene albedo and depth from a single foggy image," in *Proc. IEEE ICCV*, Sep. 2009, pp. 1701–1708.
- [23] C. O. Ancuti and C. Ancuti, "Single image dehazing by multi-scale fusion," *IEEE Trans. Image Process.*, vol. 22, no. 8, pp. 3271–3282, Aug. 2013.
- [24] H. Horvath, "On the applicability of the koschmieder visibility formula," *Atmos. Environ.*, vol. 5, no. 3, pp. 177–184, Mar. 1971.
- [25] C. Ancuti, C. O. Ancuti, C. De Vleeschouwer, and A. Bovik, "Night-time dehazing by fusion," in *Proc. IEEE ICIP*, Sep. 2016, pp. 2256–2260.